### Referee comments (questions) are in blue

### Author comments (replies) are in black

### Modifications made in the new manuscript by the authors are in red

I refer to line numbers in the track-change version of the manuscript

# Replies to Referee #2

I thank the authors for addressing my comments, I am satisfied with the vast majority of revisions and my impression is that the paper is in a very good shape now. The authors have produced a robust and very exciting dataset.

I recommend publication -- pending a couple specific comments on small parts of the manuscript that can be easily expanded a bit, and would strengthen the study further:

Note that I refer to line numbers in the tracked-changes version of the document.

AC : We thank referee #1 for their feedback and referee #2 for their additional reviews and suggestions. Figure 4 was added to compare perfectly co-located Mie and Rayleigh winds within the cloud mask. We also clarified Fig. 6 and added a panel c) in Fig. 12 to introduce the cloud top wind shear. In accordance with the suggestions of the editor, Figs. 11 and 13 (previously Figs. 10 and 12) along with Figs. A2 and A3 were reproduced using a colour scheme that is more suitable for readers with colour vision deficiencies. Please see the detailed response to the comments below.

## Specific comments:

1)

I still miss a little bit more information on what exactly is being substituted by u_cloud in the allsky product.

1.1)

New text in l.418-420: "This small systematic difference is reassuring as the winds are perfectly co-located in the cloud, however, the standard deviation of the differences is quite large at 5.38 m/s"

RC on l.415-424 and Fig. B2:

--> To be sure about the source of std of the differences that you mention in this paragraph, a 2-dimensional pdf would be more informative:

I.e. probability density estimate (or simply a scatterplot) relative to:

Mie winds retrieved in cloudy sky (e.g. x-axis) vs Rayleigh winds that were substituted (y-axis). -- or alternatively vs the difference from Rayleigh winds.

AC: New Fig. 4 shows Rayleigh winds vs Mie winds when they both coexist within the cloud mask

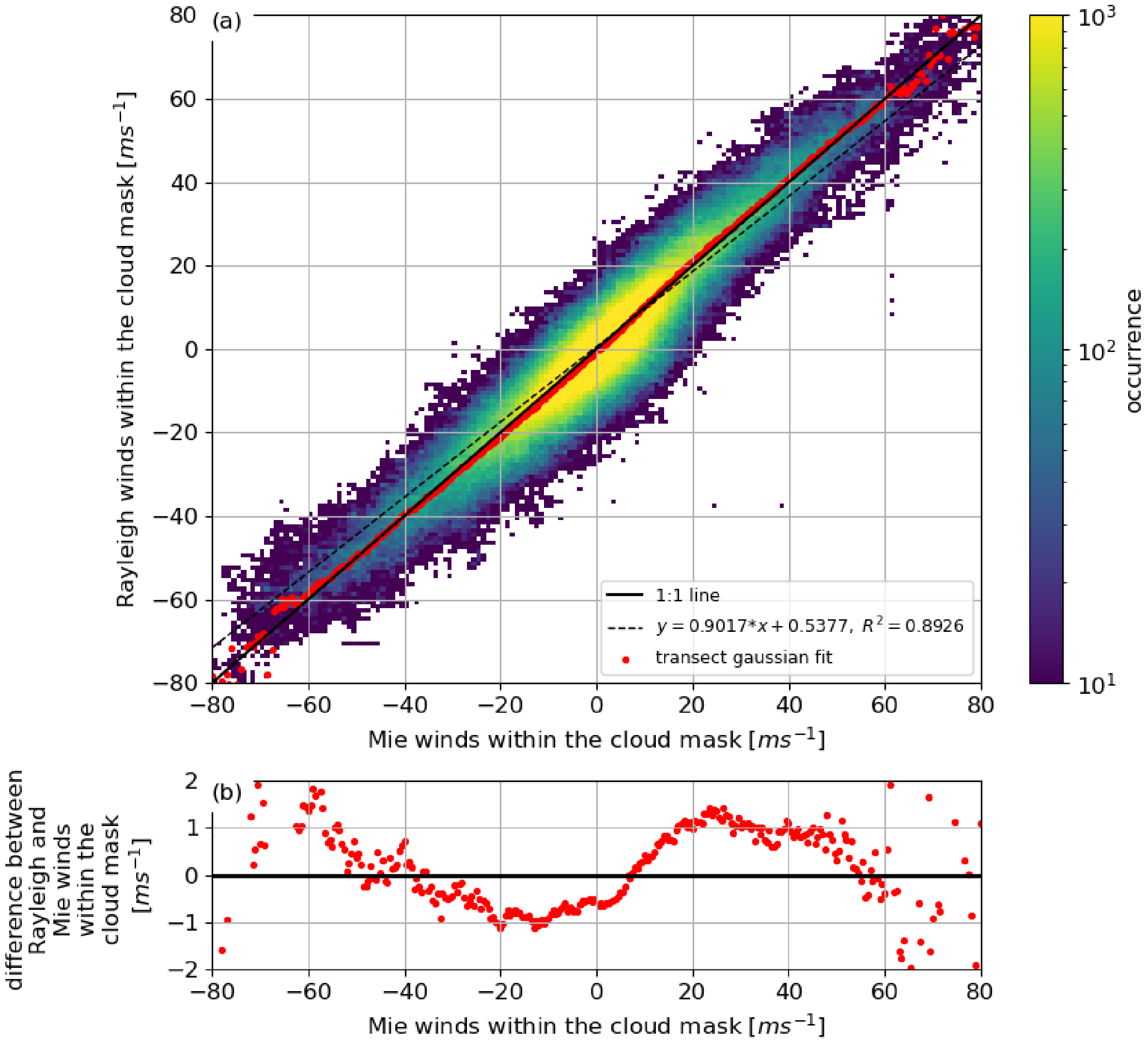


**Figure 4: (a) 2D-PDF of pairs of colocated Mie winds and the Rayleigh winds when they both coexist within the cloud mask. The black dotted line represents the best linear regression. The 1:1 line is represented as a solid black line. For each point along this 1:1 line, a Gaussian was fitted to all data points lying along a perpendicular transect. Where the data spread and statistics allow a satisfactory fit, the maximum of the Gaussian is plotted as a red filled circle each 0.5 ms$^{-1}$. (b) Maximum of the Gaussian of the differences between Rayleigh and Mie winds within the cloud mask as a function of the Mie winds within the cloud mask. A sample of 50 orbit files of the year 2020 are analysed with a total of $10^6$ bins of 3 km x 480 m where both Rayleigh and Mie winds coexist within the cloud mask.**

Does spread (std) happen around the 1:1 line (zero-line if you use differences), or is the slope different from 1 (zero if you use differences), i.e. does one dataset underestimate the magnitude of positive/negative wind regimes? Note in the latter case, the differences still can average out .

AC: The following paragraph was added at the end of Sect. 3.1, lines 323-332:

"Figure 4a shows the 2D-PDF of pairs of colocated Mie winds and Rayleigh winds which coexist within the cloud mask. The distribution is located around the 1:1 line for the entire range of wind speed, and particularly between -50 and 50 $ms^{-1}$ (98.8% of the values). For Mie wind speed between -40 and 10 $ms^{-1}$, we systematically observe Mie winds up to 1 $ms^{-1}$ larger than the co-located Rayleigh winds (Fig. 4b). For wind speeds between 10 and 50 $ms^{-1}$, the systematic differences switch signs and Rayleigh winds are up to 1 $ms^{-1}$ larger than the co-located Mie winds (Fig. 4b). For most of the wind speed values encountered in the troposphere, pairs of co-located Mie and Rayleigh winds within the cloud mask agree well, with systematic differences below 1 $ms^{-1}$ (similar to the maximum bias of Rayleigh winds, Aeolus DISC, 2024). The large spread is essentially caused by the random error of Mie and Rayleigh winds. Therefore, given the finer spatial resolution, lower random and systematic errors of Mie winds, it is preferable to substitute Rayleigh winds by the Mie winds within the cloud mask, especially for the study of wind-cloud interactions."

and removed the following lines which used to describe the 1D-PDF

"~~For cloudy bins where both Mie winds and Rayleigh winds coexist, the average difference between Mie and Rayleigh wind is -0.20 $ms^{-1}$ from June to August 2020 (Fig. B2). This small systematic difference is reassuring as the winds are perfectly co-located in the cloud, however, the standard deviation of the differences is quite large at 5.38 $ms^{-1}$. This is essentially a consequence of the random error on wind observations (approximately 5 $ms^{-1}$ for the Rayleigh winds and 3 $ms^{-1}$ for the Mie winds) and the (at least) 5 times finer native horizontal resolution of the Mie winds compared to the Rayleigh winds. The substitution of Rayleigh winds by Mie winds in cloudy sky will therefore improve the study of wind-cloud interactions.~~"

We added two sentences in the conclusion lines 878-880 :

"We showed that perfectly colocated Rayleigh and Mie wind values agree well within the cloud mask with differences below 1 $ms^{-1}$. As Mie winds have a better spatial resolution, lower systematic and random errors than Rayleigh winds, we substituted Rayleigh wind values by Mie wind values within the cloud mask."

Even in the extreme case where you have a distribution of Mie winds, and another distribution of near-zeros, you can get a PDF of the differences very similar to the one in Fig.B2. Note in Fig. 5 your values are within +-20m/s.

Important notes on this:

a) no additional data processing needed for addressing this, just plotting the data in a different way and adding a fit.

b) if such a figure is produced (showing a 2D pdf), it's worth adding it to the main manuscript: whether both winds agree well (little systematic difference despite high std), or whether the slope deviates from the expected agreement, both outcomes are an important result to show.

1.2)

Fig.5 (now Fig. 6):

in d) within the cloud mask there are actually still some u_clear values, correct?

AC : There are no u_clear in the cloud mask but there are indeed Rayleigh wind values in the cloud mask. By definition (lines 368-370), u_clear does not contain any Rayleigh wind values within the cloud mask as they are all substituted by Mie wind values when available and by no wind value otherwise.

I still miss a little bit more information on what exactly is being substituted by u_cloud in the allsky product."

Since the mask is shown with the black contours, I would ask to show the u_clear values that may exist within the mask in d).

As a reader, I'd like to see what exactly is being substituted by u_cloud in the allsky product.

--> This would really visualize and complement what is contained in the current Fig. B2: even if one gets a sense of little systematic differences, you should highlight that the cloudy part adds significantly to the dataset.

--> You mention earlier that "83% of... bins flagged as cloudy... contained both a Rayleigh and a Mie wind", and it's in this figure that you can describe how reliable Rayleigh is (compared to Mie), the deeper you go into the cloud (from the top).

AC : To clarify what exactly is being substituted by u_cloud in the allsky product, we built a new Fig. 6 (previous Fig. 5), which now contains all Rayleigh wind values (Fig. 6c) and Rayleigh winds only outside of the cloud mask, named u_clear (Fig. 6d). Accordingly, we also display all Mie wind values (Fig. 6e) and Mie wind values only within the cloud mask, named u_cloud (Fig. 6f). Figure 6g is u_allsky, the merging of u_clear and u_cloud.

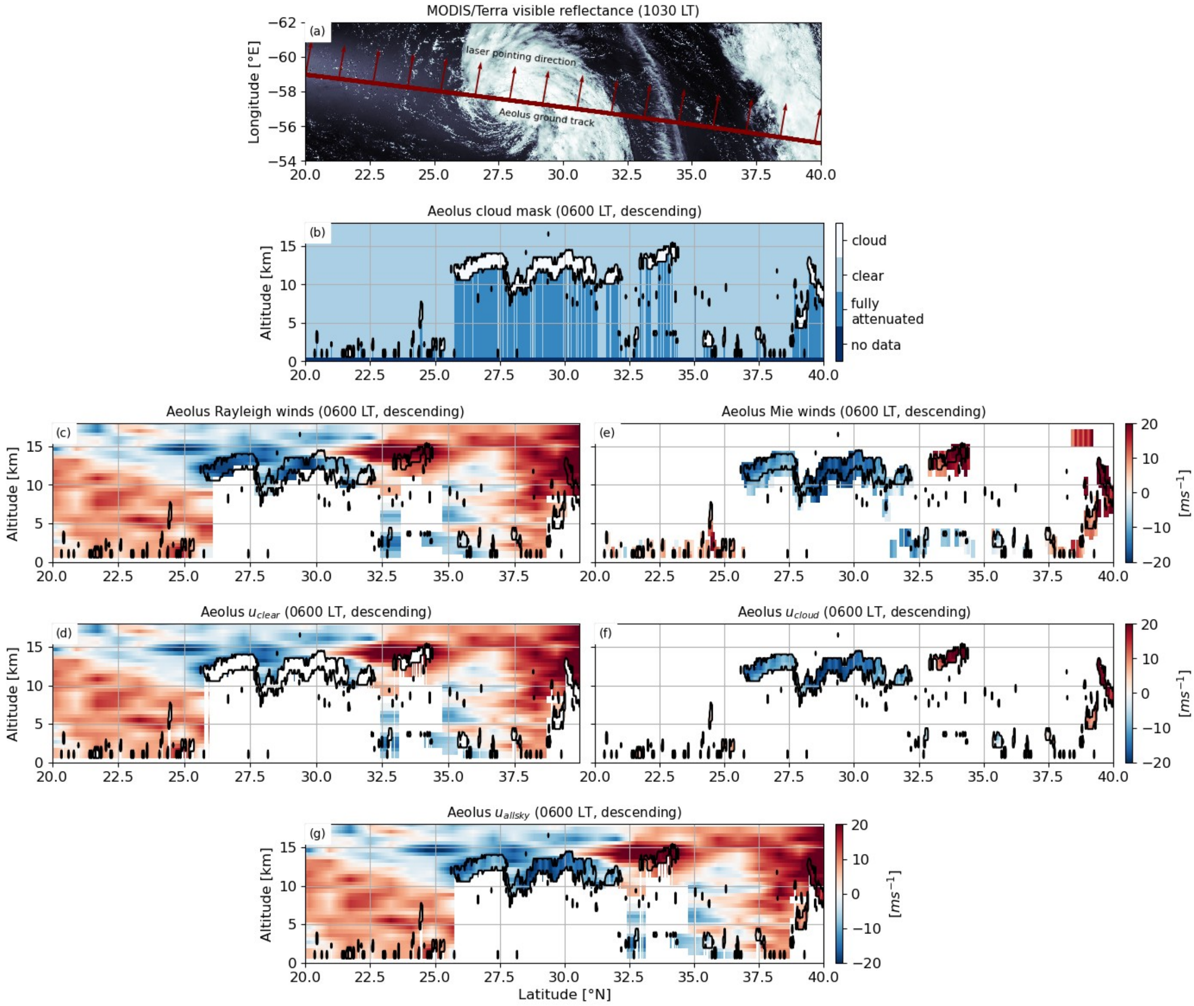


**Figure 6: (a) Descending orbit segment crossing the tropical cyclone Paulette over the Atlantic ocean (2020-09-12T09–2020-09-12T11) plotted in red over a MODIS/Terra reflectance image. The red arrows represent the laser pointing direction. (b) Aeolus cloud mask. Aeolus (c) all Rayleigh winds and (d) Rayleigh winds only outside of the cloud mask, noted u_clear along the paper. Aeolus (e) all Mie winds, (f) Mie winds only within the cloud mask, noted u_cloud along the paper. (g) All-sky winds, noted u_allsky, result from the merging of u_clear and u_cloud. The winds are negative when blowing westward and positive when blowing eastward. For panels (b-g), the resolution of the re-sampled data is 3 km horizontally and 480 m vertically and the black contour is the cloud mask.**

We revised the final paragraph of Sect. 3.3, lines 464-489:

"Figure 6 illustrates how Aeolus resampled cloud mask and winds allow us to observe from space different features ranging from cyclones to cumulus clouds. During its lifetime, Aeolus observed multiple cyclones, sometimes crossing them near their centre (Marinescu et al., 2022). Figure 6a shows an example of intersection between Aeolus and the tropical cyclone Paulette over the Atlantic Ocean during the hurricane season, on 12 September 2020. The wind and cloud curtains are displayed between 20°N and 40°N (Fig. 6b-g). Note that Aeolus covers this distance in about 4 minutes, so the curtains represent a snapshot of the scene. The cyclone is identified by the continuous high cloud cover between 26°N and 32°N at about 12 km of altitude (Fig. 6b). The laser typically only penetrates 1 to 2 km below the uppermost cloudy layer of the cyclone. This particular case study is also interesting as it encounters a diversity of clouds. We observe a cirrus cloud, northward of the cyclone, extending from 33°N to 34°N and between 12 and 15 km of altitude. Along half of its length, this cirrus does not fully attenuate the laser as some clear sky layers can be retrieved below its base. We also observe shallow cumulus clouds (Fig. 6a, 6b) between 20°N and 26°N, with their tops below 3 km of altitude and sometimes only occupying a single profile, surrounded by clear sky profiles. This stresses out the importance of performing cloud detection at full horizontal resolution of 3 km. ~~allowing us to observe the cloudy sky winds at the top of the cyclone, near the outflow level (Fig. 6c).~~ Aeolus retrieves Rayleigh winds above and around the cyclone, up to 18 km of altitude (Fig. 6c). As the horizontal resolution of Rayleigh winds is fixed to 87 km, and molecular signal is still retrieved within clouds, some Rayleigh winds can be retrieved within clouds. For example, there are Rayleigh winds within the upper cloudy layers of the cyclone and in the entire boundary layer, even within shallow cumulus clouds (Fig. 6c). However, we only keep Rayleigh wind values outside of the cloud mask when building $u_{clear}$ (Fig. 6d). The cross section of $u_{clear}$ (Fig. 6d) reveals the wind shear found where counter-clockwise winds around the cyclone base meet the clockwise winds at the top of the cyclone. This happens at about 8 km of altitude at 25°N and at 35°N. The further we look from the cyclone, the higher in altitude the reversal of the wind occurs. Figure 6e shows the Mie winds retrieved by Aeolus. Most Mie winds are retrieved within the cloud mask. As the native resolution of Mie winds can be as coarse as 15 km, it is possible that Mie winds extend horizontally beyond the cloud mask as shown around shallow cumulus clouds, between 20°N and 26°N, below 3 km of altitude (Fig. 6e). $u_{cloud}$ (Fig. 6f) contains only Mie winds values within the cloud mask (as detailed in Sect 3.1). The merging of $u_{clear}$ and $u_{cloud}$ constitutes the all-sky wind, $u_{allsky}$ (Fig. 6f)."

2)

Response to specific comment 6

"The referee is right to point out that adding the information about S at the cloud top and above would be very interesting. We plan to do it in a following study dedicated to specific cloud types and associated scientific questions".

RC: I'd still suggest adding it -- including this would require very little work, as the parameter is already calculated, and it wouldn't really take much from your follow-on study. On the contrary I think it would strongly motivate the mentioned follow-on study. While reading this section of the paper this is the first thing that pops in my mind as a tiny missing element that would strengthen and complement the section a lot.

-- Having said the above, it's also not a critical part of the study so I'm fine if the Editor does not deem it necessary.

Cloud top wind shear profiles are added in the new panel c) of Fig. 12 (previously Fig. 11) and occurrences of cloud top wind shear measurements at each altitude are added in Fig. B10. We also updated Fig. B9 accordingly to describe where and how the cloud top wind shear $S_{cloud\_top}$ is computed.

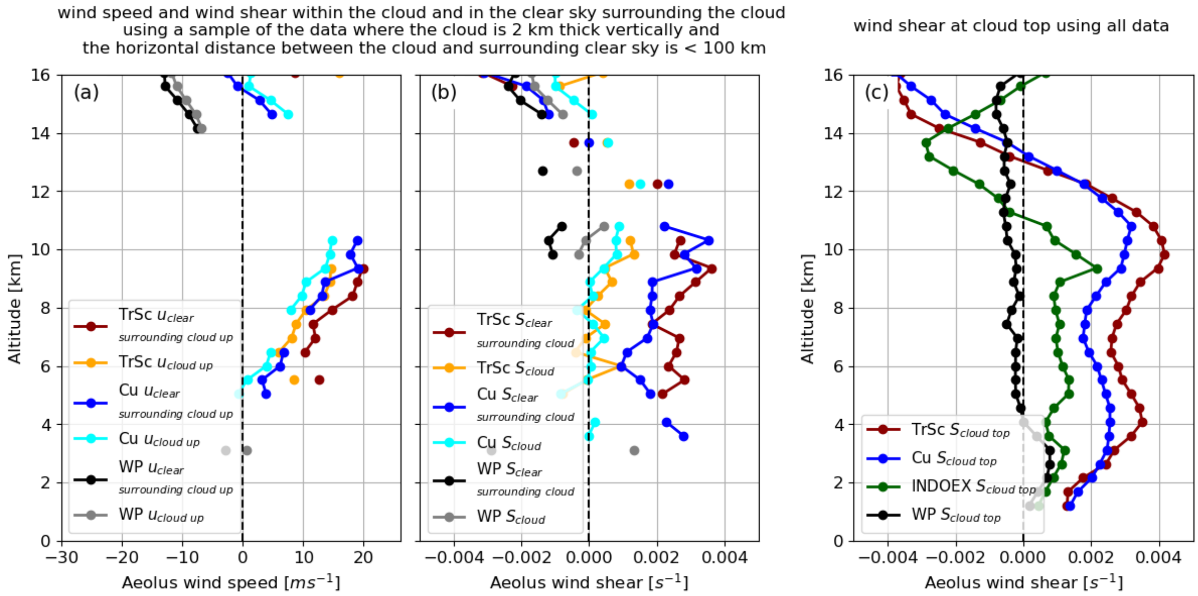


**Figure 12: (a) average wind speed profiles retrieved within the uppermost cloudy layer $u_{cloud\ up}(z)$ and average of the closest clear sky wind speed $u_{clear\ surrounding\ cloud\ up}(z)$ observed over each region. Only values where $u_{cloud\ up}(z)$ and $u_{clear\ surrounding\ cloud\ up}(z)$ are significantly different (two sided T-test with p-value < 0.05) are plotted. (b) Average wind shear profiles within the cloud $S_{cloud}(z)$, and in the surrounding clear sky $S_{clear\ surrounding\ cloud}(z)$ are computed at each altitude z using the the wind speed observed at $z_1$ located 1 km below z and at the wind speed observed at $z_2$ located 1 km above z. Note that for (a) and (b), only a sample of the data is used as each cloud should be at least 2 km thick vertically, and the horizontal distance between $S_{cloud}(z)$ and $S_{clear\ surrounding\ cloud}(z)$ must be < 100 km and only values where $S_{cloud\ up}(z)$ and $S_{clear\ surrounding\ cloud\ up}(z)$ are significantly different (two sided T-test with p-value < 0.05) are plotted. (c) Average cloud top wind shear $S_{cloud\ top}(z)$ profiles retrieved in each region during the year 2020 using all data collected by Aeolus over each region contrarily to (a) and (b) that use only a sample of the data.**

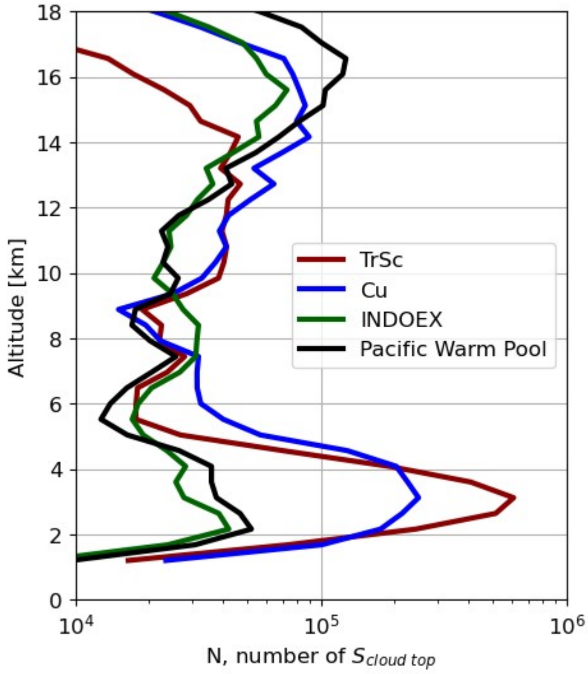


**Figure B10: Occurrences of cloud top wind shears over each region**

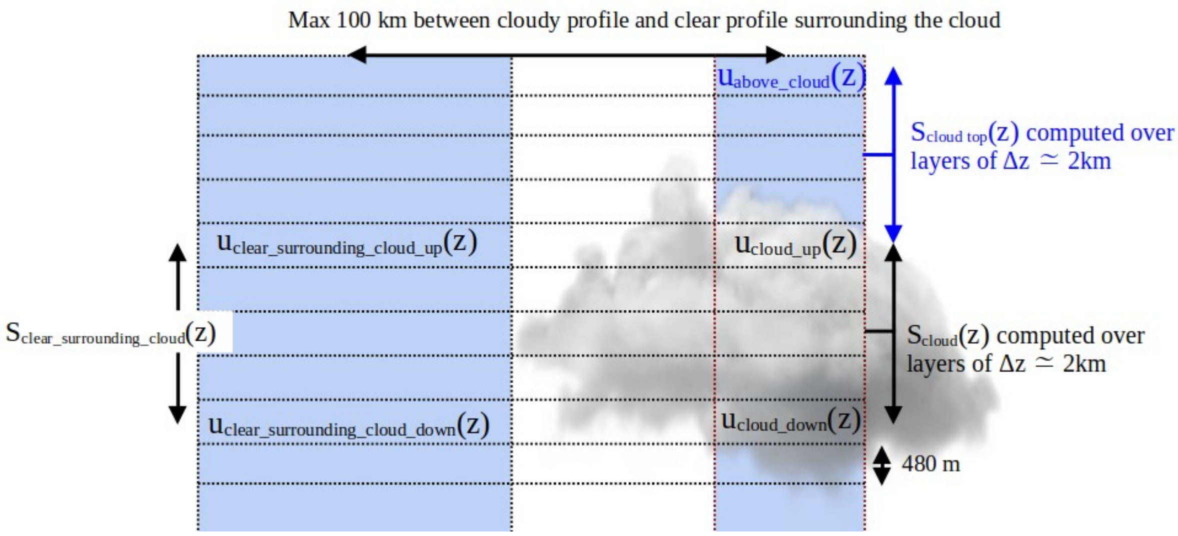


**Figure B9: complements relative to the calculations of wind shears for Fig. 11. For each profile containing a cloud, we compute $S_{cloud\_top}(z)$ the wind shear between the clear sky above the cloud and the uppermost cloudy layer. We extract a sample of these profiles which has to respect two conditions : the cloud must be at least 2 km thick vertically, and there must be clear sky in the surrounding, within a distance of 100 km. We compute $S_{cloud}(z)$ the wind shear within the cloud, and $S_{clear\_surrounding\_cloud}(z)$ the wind shear in the surrounding of the cloud. Wind shears are calculated over 2 km thick layers.**

We added the following paragraph in the revised manuscript in Sect. 4.3.3, lines 798-809:

"By retrieving the wind both within clouds and above cloud tops, this Aeolus dataset gives access to the wind shear at the top of the clouds (Fig. 12c). Note that to study the wind shear at the top of clouds (Fig. 12c), we analyse all the data collected over each region contrarily to Fig. 12a and 12b. Within each region, we record the wind speed observed in the uppermost cloudy layer (noted $u_{cloud\_up}$) and the clear sky wind speed 2 km above (noted $u_{above\_cloud}$). We then compute $S_{cloud\_top}$, the wind shear between these two layers (see Fig. B9). Figure 12c shows the average profile of $S_{cloud\_top}(z)$ for the different regions. Within the lower troposphere, the largest number of cloud top wind shear observations is found between 2 and 3 km of altitude over the TrSc and Cu regions (Fig. B10), which is consistent with Wood (2012) and Cesana et al., (2019). At these altitudes, the average wind shear at cloud top $S_{cloud\_top}(z)$ ($2\times10^{-3}$ to$3\times10^{-3}$ $s^{-1}$, Fig. 12c), is larger than in all sky conditions $S_{allsky}(z)$ (about $1.5\times10^{-3}$ $s^{-1}$, Fig. 11c). This result is consistent with previous work stating that a temperature inversion above cloud tops isolates the cloudy layer from the clear sky above. A zone of larger wind shear can thus develop around the temperature inversion (Wang et al., 2008; Hourdin et al., 2019), which can in turn affect the morphology of these clouds through entrainment and drying of the boundary layer (Schulz & Mellado, 2018; Zamora Zapata et al., 2021)."

We added a sentence in the conclusion, lines 902-903:

"We also found that the observed cloud top wind shear above Stratocumulus and Cumulus clouds ($2\times10^{-3}$ to $3\times10^{-3}$ $s^{-1}$) was larger than the observed all-sky wind shear at the same altitude ($1.5\times10^{-3}$ $s^{-1}$)."

## Minor/technical comments:

1)

Figure AC2.1:

This would be a very welcome addition to the supplement. Please specify in the main manuscript -- when discussing Fig.7 -- that for completeness you show absolute shear values in the appendix.

Fig. B11 was added in the Appendix as well as the formula to compute the absolute wind shear. This new figure is mentioned in the manuscript in Sect. 4.1, line 547: "Note that a similar map, but with absolute wind shears is shown in Fig. B11."

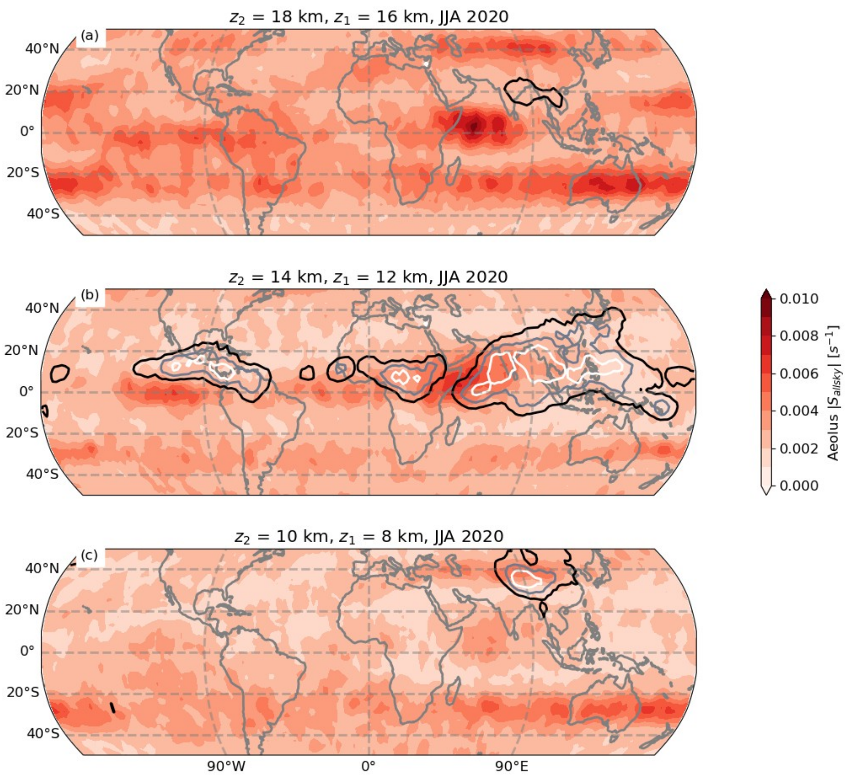


**Figure B11: Map of the median absolute wind shear $|S_{allsky}|$ calculated a) between 8 km and 10 km, b) between 12 and 14 km and c) between 16 and 18 km from June to August 2020. Contours represent cloud covers of 5, 10, 15 and 20% for each altitude range.**

2)

l.343-345: reference needed, need to be specific about which of the above references are the latest you refer to.

Reference to the latest Aeolus DISC report was added in Sect. 3, lines 253-255 :

"The latest validation report of Aeolus showed systematic error (bias) of below 0.5 ms-1 for Mie winds and below 1 ms-1 for Rayleigh winds, while the random error is about 3 to 4 ms-1 for Mie winds and 3 to 6 ms-1 for Rayleigh winds (Aeolus DISC, 2024)."

and replace the old version that was in the track change manuscript : "~~The latest validation campaigns of Aeolus showed that the systematic error (bias) for wind measurements remained within the mission requirements of 0.7 ms-1 for both Mie and Rayleigh channels, while the random error was about 3 ms-1 for the Mie channel and 5 to 7 ms-1 for the Rayleigh channel.~~"

3) Perhaps I missed it, but now the INDOEX region is no longer included in Fig. 11 (now Fig. 12, Fig.10 in previous manuscript version) and I can't seem to find any note/reference/justification for that change.

Correct. The INDOEX region is no longer visible in Fig. 12 as there are no altitudes at which both $u_{cloud\_up}$ and $u_{clear\_surrounding\_cloud\_up}$, $S_{cloud}$ and $S_{clear\_surrounding\_cloud}$ are significantly different. We now mention in the text why INDOEX is not visible in Fig. 12 in Sect. 4.3.2, lines 779-781 : "Note that over the INDOEX region, there are no altitudes where $u_{cloud\_up}(z)$ and $u_{clear\_surrounding\_cloud\_up}(z)$ are significantly different and where $S_{cloud}(z)$ and $S_{clear\_surrounding\_cloud}(z)$ are significantly different, hence this region does not appear in Fig. 12a and Fig. 12b."

4)

l.665-680: please add a little bit of discussion regarding shear, use the Jensen reference here already (you name it in the next subsection)

We added two pieces of discussion regarding Fig. 8. In Sect. 4.1 lines 555-557 :

"Jensen et al., (2025) demonstrated that wind shears of $10\times10^{-3}$ $s^{-1}$ were favourable for a faster sublimation of cirrus clouds particles, reducing the lifetimes of these clouds."

you may add also e.g. Schaefler et al. (2020) https://doi.org/10.1175/MWR-D-19-0229.1

e.g. are your magnitudes of shear near the jets close to their Fig. 9?

and in Sect. 4.1 lines 571-577 :

"At the North bound of the map, at about 50°N, the tropopause layer is located between 9 and 10 km of altitude at the end of boreal summer (Schäfler et al., 2020). We observe a wind shear of about $1\times10^{-3}$ $s^{-1}$ around the globe at this latitude (Fig. 8c). Indeed, the wind profile is tilted eastward below the tropopause and westward above, which explains the weak positive wind shear around the tropopause. Schäfler et al., (2020) reported a weak, but negative wind shear of $-1\times10^{-3}$ $s^{-1}$ between 8 and 10 km for the month of October at about 60°N. The change of sign might be explained by a lower altitude tropopause at 60°N, 10 degrees northward of our observations, and thus by a larger contribution of the westward tilted profile above the tropopause."

Note that to derive the wind shear from Schäfler et al., 2020, we used the average over all flights (their Fig. 1) rather than the case study (their Fig. 9).

5)

l.906-907: "This suggests an important role...": sentence too vague, and wind shear role on convective organization is well known. Can be removed, or expanded with proper referencing.

We removed the following sentence in Sect. 4.3.2, line 734: "~~This suggests an important role of wind shear in limiting the vertical extent of convection.~~"